High-speed *in vitro* intensity diffraction tomography: supplementary material

Jiaji Li[a,b], Alex Matlock[a], Yunzhe Li[a], Qian Chen[b], Chao Zuo[b,*], and Lei Tian[a,*]

[a]School of Electronic and Optical Engineering, Nanjing University of Science and Technology, Nanjing, Jiangsu 210094, China
[b]Department of Electrical and Computer Engineering, Boston University, Boston, MA 02215, USA
[*]zuochao@njust.edu.cn, leitian@bu.edu

ABSTRACT

This document provides supplementary information to "High-speed *in vitro* intensity diffraction tomography". We provide more details including: intensity diffraction tomography technique utilizing annular illumination (aIDT) transfer function analysis, aIDT illumination calibration method, experimental details and tomographic RI reconstruction of Spiral algae and fixed *C. elegans*.

Correspondence to: Lei Tian, leitian@bu.edu

1 aIDT Transfer Function Analysis

In our aIDT system, an LED ring is used for the illumination in a standard brightfield microscope (E200, Nikon). 24 LEDs are uniformly arranged on the ring-shaped circuit board. Each LED provides a plane wave of unique angle. We match the illumination numerical aperture NA_{illum} to the objective NA NA_{obj} (i.e. NA_{illum}=NA_{obj}). According to our theory [30], the absorption and phase transfer functions (ATF, and PTF, respectively) both contain a pair of circular Fourier regions describing the scattered field's information and its complex conjugate. Figure S1 shows a few representative examples of the ATF, PTF, the corresponding experimentally captured intensity Fourier spectrums, and the central slice of PTF Fourier coverage. The objective pupil is shifted by the oblique illumination such that the two pupil areas are next to each other. As illustrated in Fig. S1(a), the overlap between the two circular regions of PTF will cancel the captured low spatial frequency information, and the zero region can be completely eliminated by matching NA_{illum} to NA_{obj}. By varying the illumination angle, the location of the pupil position changes accordingly. The two circular regions contain minimal overlap and ensure optimal simultaneous low and high frequency information coverage. To enable the dynamic live imaging, we can reduce the measurement acquisition by downsampling the total LED number and make a tradeoff between the imaging quality and speed. With the increasing of illumination LED number, the PTF can provide $2NA_{obj}$ imaging resolution and better non-zero region Fourier coverage in all directions. Together, our annular illumination scheme enables capturing both phase and absorption information in 3D using a small number of intensity-only measurements. More details for demonstrating the operation of the system is provided in Video 1.

2 aIDT Illumination Calibration Method

For the illumination calibration method in aIDT, we also demonstrate this method on an LED matrix. The annular illumination pattern is displayed on the LED matrix (64×64, Pixel Pitch 1.25 mm), and we adjust the height of LED array to match the illumination pattern with the objective pupil (40×, 0.65 NA). The annular pattern on the LED array contains 120 LEDs and the intensity images are captured under each illumination angles. The uncalibrated spatial frequency positions of all LEDs are plotted in the blue stars in Fig. S2(a). We first applies the algorithm in previous work [36] to provide initial LED position estimates, whose results are shown in the red dots in Fig. S2(a). In practice, this algorithm [36] is subjected to noise. As a result, the calculated LED positions can be placed outside of the square grid from the LED matrix, as shown in the enlarged region in Fig. S2 (problematic regions are marked in the red arrows). Next, we incorporate the geometric constraints to refine the LED positions by applying a nonlinear fitting algorithm, whose results are shown in the green triangles in Fig. S2(b). In Fig. S2(c-g), we also provide the experimentally captured intensity Fourier spectrum and their corresponding LED's spatial frequency position. The shifted objective pupil is marked by the circles in Fig. S2(c-g) (uncalibrated pupil marked in blue circles, calibrated pupil marked in green circles).

3 Experimental Details

The image acquisition and data processing time are different for imaging static and living samples. All fixed samples are reconstructed by capturing 24 intensity images; the live *C. elegans* are imaged with 8 frames due to the fast dynamics. The exposure time is 25ms for the fixed samples and 4.4ms for *in vivo* observation. All the processing are done using MATLAB (MATLAB R2018a) on a personal computer (Intel Core i7-8700K, 3.7 GHz, 64 GB DDR4 RAM). The computation time to perform LED position calibration (for 400×400×24) is about 2 seconds. 3D reconstruction time for a 1024×1024×51 RI stack takes about 50 seconds. Importantly, the volumetric reconstructions are performed based on 2D FFTs instead of 3D FFTs due to the slice-wise model. The processing time of 3D reconstruction can be significantly reduced from several tens of seconds to a few hundreds of milliseconds by harnessing the power of the graphics processing unit (GPU, e.g. NVIDIA's CUDA parallel computing architecture). The reconstructed 3D RI is rendered using an open source software, Fiji [43].

As for sample preparation, for buccal smear, the fresh human buccal epithelial cells are placed in the gap between the coverslips and glass slide with 0.9% sodium chloride matching solution (n_m = 1.33). For *C. elegans* preparation, the worms were mounted on 3% agarose pads in a drop of nematode growth medium (NGM) buffer. A solid pad was made with 3% agarose in NGM buffer and placed onto the slide. Then a drop of liquid NGM buffer was applied on top of the agarose pad, and young adult *C. elegans* were added to this liquid drop. Glass coverslips were then gently placed on top of the pads and sealed with a 1:1 mixture of paraffin and petroleum jelly [47,48]. The RI of liquid NGM buffer medium inside slit is 1.33, which is similar to water due to low salt concentrations.

4 Tomographic RI Reconstruction of Spiral Algae

Here, we provide additional tomographic RI reconstruction on a stained spiral algae sample (S68786, Fisher Scientific) using the 10× objective (0.25 NA) to demonstrate the capability of the proposed method to image absorbing object. By simply adjusting the LED ring height, we first match the illumination NA with the 0.25 NA, 10× objective pupil aperture. Next, we capture 24 intensity images to reconstruct the 3D complex permittivity distribution. The slice spacing of the reconstruction is set to be 5μm. A sample full field of view brightfield image of the spiral algae sample is illustrated in Fig. S3. Next, we show tomographic reconstruction by zooming the central region. The reconstructed slices, containing both the real (phase) and imaginary (absorption) part of the refractive index are shown in Fig. S3(c) ranging from -85μm and 85μm. It is highlighted that the dense algae clusters are successfully resolved in the refractive index reconstruction and the small "phase" features (filaments) at different depths are clearly distinguished from z planes ranging from 15μm to 35μm, (marked with white circles) can be resolved axially. The unstained filaments are reconstructed with high contrast in the phase reconstruction whereas the absorption reconstruction does not provide much contrast. The spiral structure on a single spirogyra is successfully reconstructed as marked by the arrows. Overall, these results demonstrate that aIDT is able to reconstruct both highly absorbing (e.g. chloroplasts) and "phase" features (e.g. filaments). The ability to resolve the spiral structure further demonstrating the axial sectioning capability of our technique. Further details of the reconstruction are provided in Video S1.

5 Tomographic RI Reconstruction of Fixed *C. Elegans*

We also apply our method to the 3D RI reconstruction of fixed *C. elegans* to demonstrate aIDT's capability in evaluating complex tissue structures. For the fixed worm sample, we captured 24 full frame intensity images (2048×2048 pixels) using the 40× objective with 0.65 NA. Figure S4 shows the tomographic RI reconstructions of two *C. elegans* at different stages of the life cycle. The two central RI slices of full worms shown in Fig. S4(a) and (d) highlight the different morphological and biological structures captured with our approach. We identify specific internal tissue features including embryos, pharyngeal bulbs, intestinal lumen, and the rectum in the marked sub-regions (red rectangular) in Fig. S4(b,c) and Fig. S4(d,e), respectively. With these axial slices, we identify the *C. elegans* in Fig. S4(a) is an adult hermaphrodite based on the presence of a developed reproductive system. The slices for the Fig. S4(d) worm show no reproductive system and a thin tail, suggesting this worm is more juvenile in the L3 or L4 development stage. Capturing this information, as well as the full digestive tract from the grinder to the intestinal lumen and rectum, enables longitudinal evaluations of tissue development within the *C. elegans*. This provides significant utility in pathology or organogenesis, where tissue development in the presence of drugs, parasites, or genetic mutations could be valuable for research and clinical applications. The worm in Fig. S4(d) is likely in the L3 or L4 stage of development [49]. This tomographic RI reconstruction of fixed *C. elegans* shows our technique enables classification of the individual worm segments and identification of the worm type as an adult hermaphrodite based on the presence of embryos and its tail structure. The whole volume RI reconstruction of *C. elegans* worms are provided in Video S2.

6 Data and code

The Matlab codes and raw experimental data in this manuscript are available on GitHub at https://github.com/bu-cisl/IDT-using-Annular-Illumination.

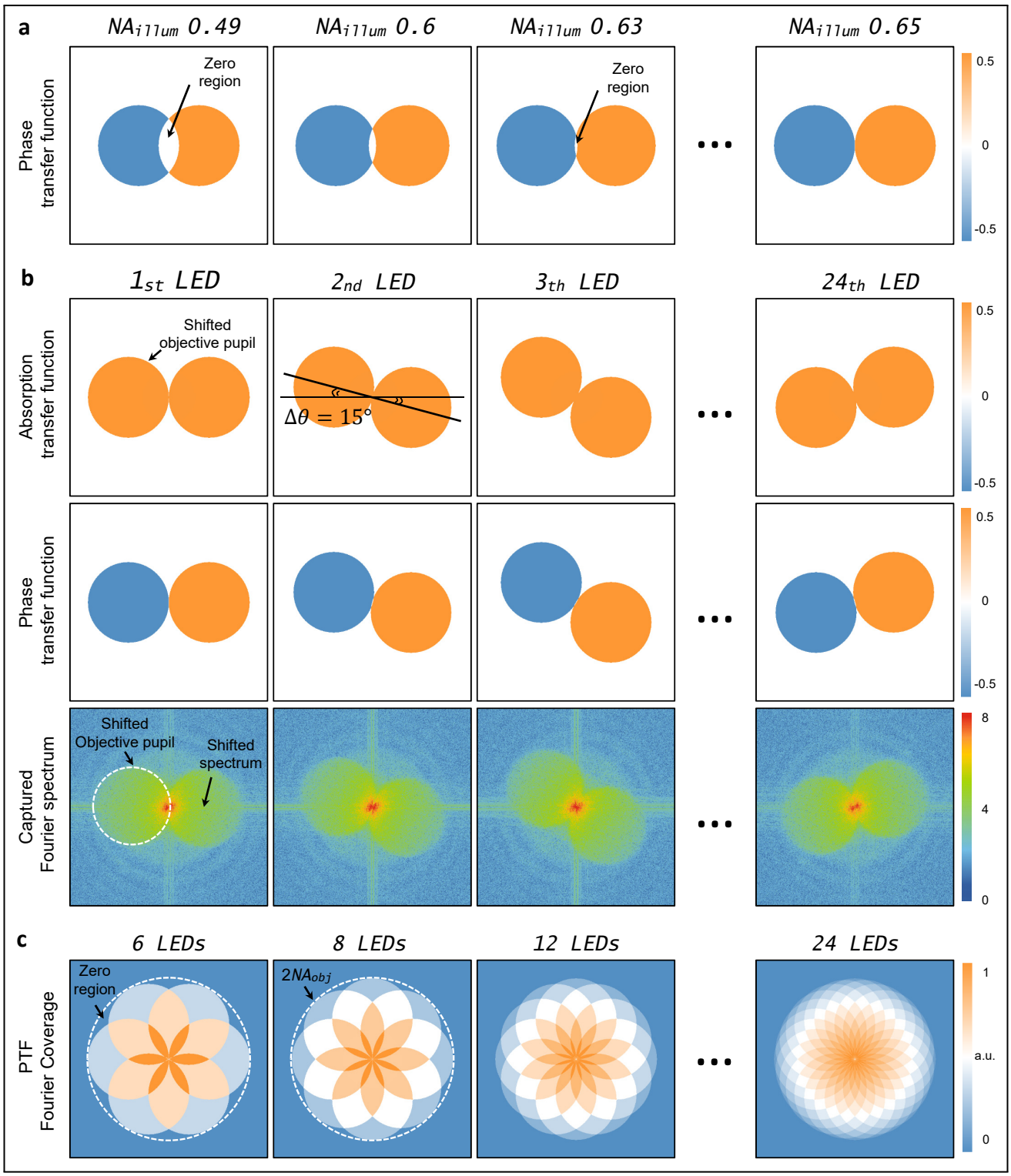

Figure S1. Transfer function illustration of aIDT. (a,b) The absorption and phase transfer functions of aIDT and the corresponding experimentally obtained intensity Fourier spectrums. (c) Fourier coverage of PTF with different illumination LED number.

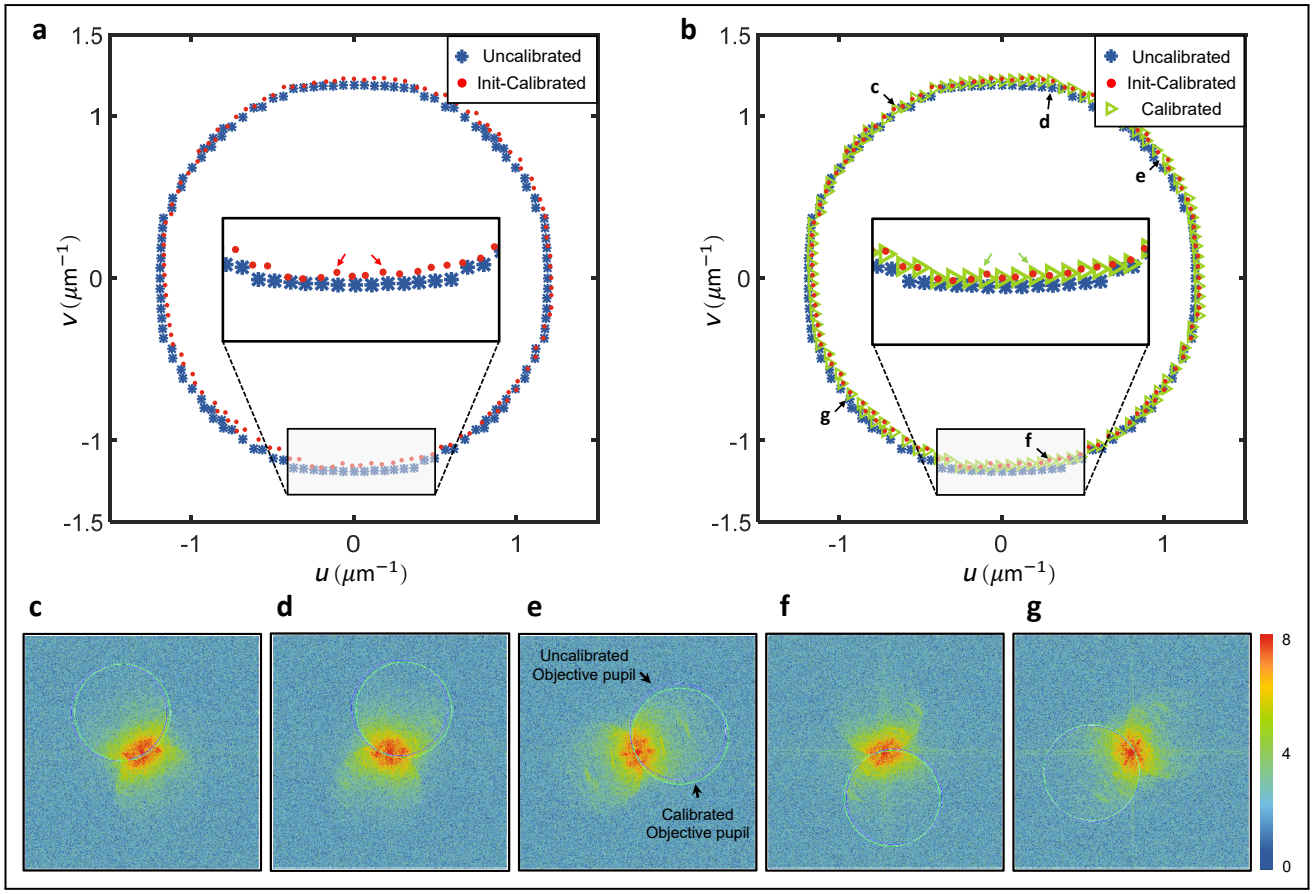

Figure S2. Demonstration of our self-calibration method on an LED matrix. (a) The LED positions from manual alignment (termed uncalibrated, marked in blue star) and initial guess of calibration (termed Init-calibrated, marked in red dot), plotted in the spatial frequency coordinates. (b) Calibrated spatial frequency positions of LEDs (green triangle). (c-g) Captured Fourier spectrum using the corresponding LED (marked with arrows) along with calibrated pupil positions (marked by circles).

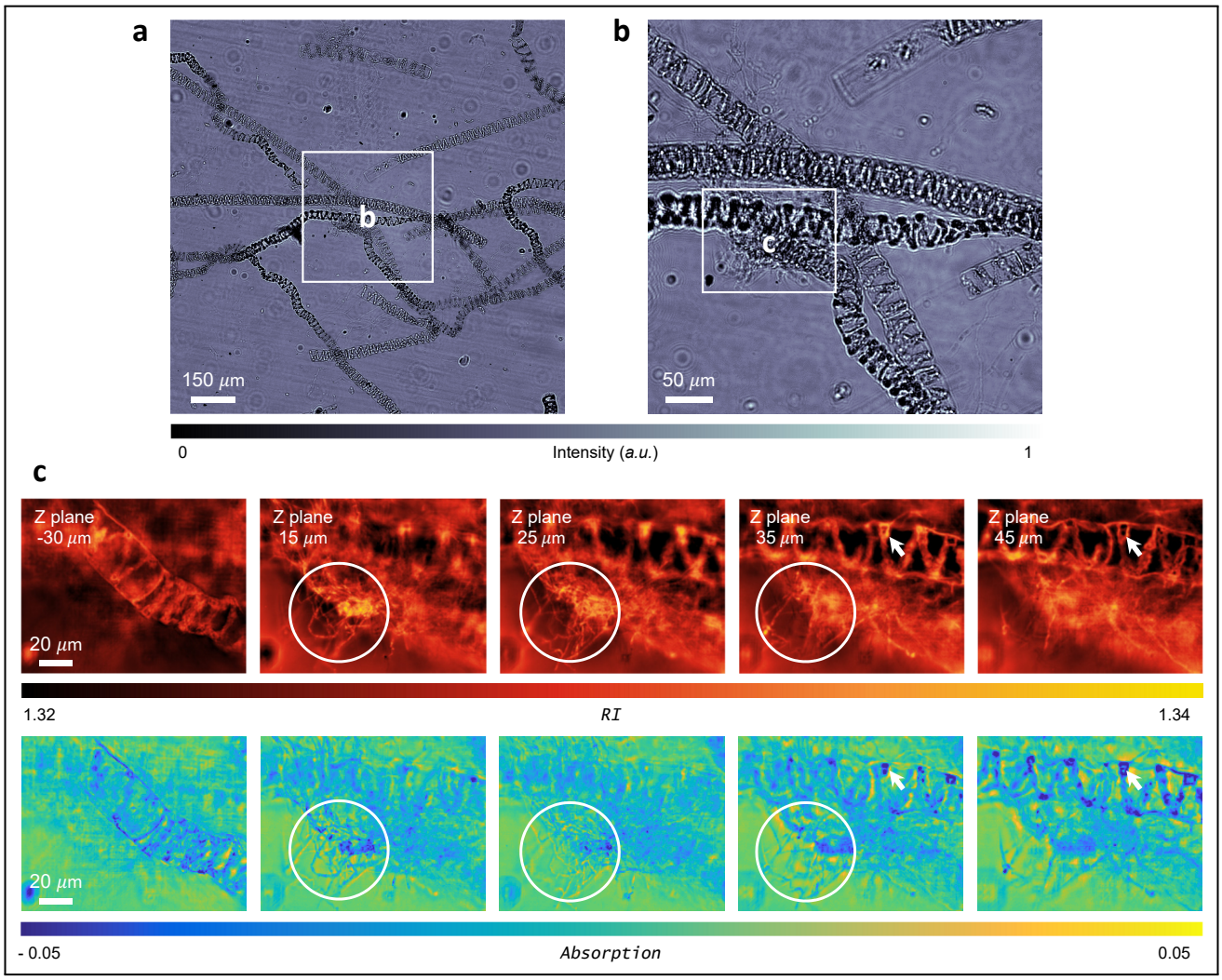

Figure S3. Phase and absorption aIDT reconstruction of stained spiral algae sample. (a,b) The full field of view and a zoom-in sub-region of the brightfield intensity image. (c) Reconstructed cross sectional refractive index at 5 axial depths. (Top) Phase, (Bottom) Absorption.

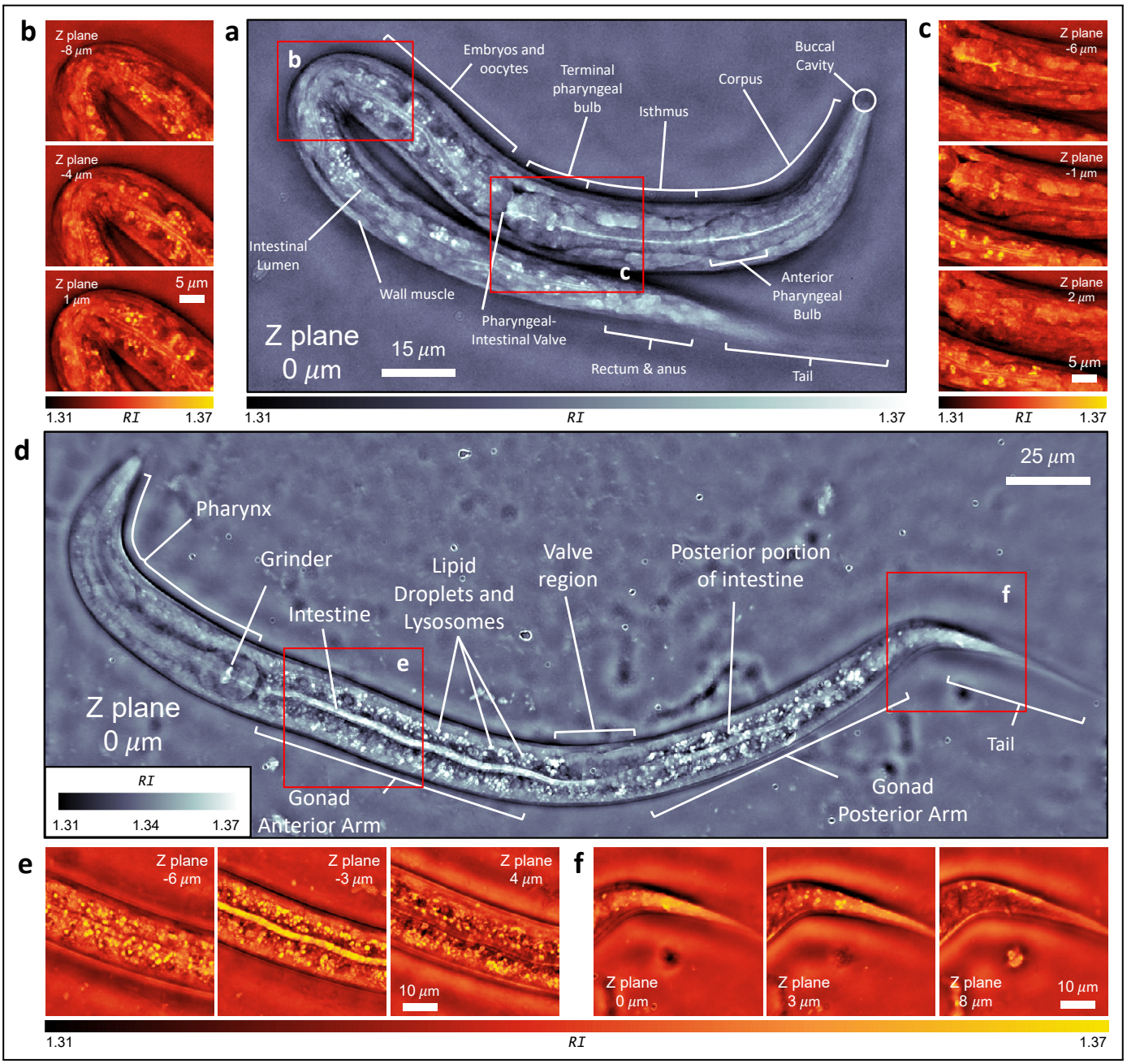

Figure S4. Tomographic RI reconstruction of fixed *C. Elegans*.